Proceedings of HTSC 2005:
Heat Transfer Summer Conference
San Francisco, CA, July 17-22, 2005

HT2005-72263

CHARACTERIZATION OF OPTICAL MICROCAVITY WHISPERING-GALLERY-MODE RESONATORS

Haiyong Quan and Zhixiong Guo*
Department of Mechanical and Aerospace Engineering
Rutgers, The State University of New Jersey, Piscataway, NJ 08854
***Corresponding Author: (732) 445-2024, guo@jove.rutgers.edu**

ABSTRACT

In the past decade, optical microcavity whispering-gallery mode (WGM) resonators have received increasing attention for applications in optical communications and nanotechnology. In this paper, the theory for describing radiation transfer and heat transfer in the micro/nanoscale devices is presented first. Then the characteristics of waveguide-microdisk coupling WGM miniature resonators are numerically studied. Focus is placed on the parametric studies over a broad range of resonator configuration parameters including the microcavity size and the gap separating the microdisk and waveguide. The finite element method is used for solving Maxwell's equations which govern the propagation of electromagnetic field and the radiation energy transport in the micro/nanoscale devices. The EM field and the radiation energy distributions are obtained and compared between the on-resonance and off-resonance cases. A very brilliant ring with strong EM field and high radiation intensity is found inward the periphery of the microdisk under resonances and high energy storage is achieved. The microdisk size affects significantly the resonant frequencies and their intervals. The scattering spectra for three different microcavity sizes are obtained. The gap obviously influences the qualify factor, the full width at half maximum, and the finesse of the resonant modes as well as the capability of energy storage.

INTRODUCTION

Advances in micro/nano-fabrication techniques have made it feasible to consider optical resonators having physical dimensions in the order of optical wavelengths. As a particular mode of microcavity resonances, whispering-gallery modes (WGMs) occur when light rays travel in a dielectric medium of circular geometry[1] like spheres, disks, rings, and cylinders. After repeated total internal reflections at the curvilinear boundary the electromagnetic field can close on itself, giving rise to resonances. Microcavity WGM resonators have high potentials for realization of microlasers,[2] narrow filters,[3] optical switching,[4] single molecule detection biosensors,[5] and high resolution spectroscopy,[6] etc.

WGM resonances are morphology-dependent. The resonant frequencies mainly depend on the size of the resonator. In general, the resonant modes are approximately predicted by $2\pi r = mc_0/(f_m \cdot n)$; where m is an integer, n is the refractive index of the resonator material, and r is the radius of the resonator. The frequency shift of a given resonant mode assuming constant refractive index is then estimated as: $\Delta f / f \approx -\Delta r / r$, where Δr represents a small change of the radius. If we consider the linewidth of the resonance to be the smallest measurable shift (taken as $\Delta f = 10$ MHz, $f = 3.75 \times 10^8$ MHz at $\lambda = 800$ nm), then the smallest "measurable" size change is $|\Delta r|_{\min} = 2.6 \times 10^{-8} r$. With a radius r = 10 μm in a typical microcavity resonator, $|\Delta r|_{\min} = 2.6 \times 10^{-4}$ nm — a value smaller than the size of an atom is potentially detectable in theory!

Such a feature can be explored for use as detectors and sensors for identifying molecules surrounding the peripheral surface of WGM resonators. When peptides, protein molecules, or cell membranes are attached on a resonator, for example, they interact with the evanescent radiation field around the resonator. The interactions polarize the molecules or target analytes and change the effective size and/or refractive index of the resonator. All these may lead to frequency shift of the resonance modes. Thus, it is possible to identify and detect molecules by observing the resonant frequency shifts in an optical microcavity WGM-based sensor.

In recent years, WGM molecular biosensors have been studied as a research field of attractive interest because of the great need in life sciences,[7-10] drug discovery, and recent worldwide protection from the threat of chemical and bio-terrorism. Usually the optical resonance techniques can be used to enhance the sensitivity of biosensor devices. WGM miniature sensors possess high sensitivity, small sample volume, and robust integrated property to make a lab-on-a-chip device[8] and can be used to identify and monitor proteins, DNA, and toxin molecules. They can detect as few as 100 molecules.[9]

In many WGM based sensing studies,[10,11] the WGM resonators are generally microstructures consisted of microspheres and eroded optical fibers.

However, the microsphere and fiber coupling design has some obvious flaws for use as ideal sensors. For instance, mass manufacture is difficult and non-uniformity exists; not to mention that it is difficult to control the gap distance between the eroded optical fiber and the microsphere which is critical for photon tunneling. In this study, we consider an innovative design of waveguide and microdisk coupling structure as the optical microcavity WGM resonator. In this design, mass manufacture can be easily achieved through nanofabrication, and the devices are of high uniformity and easy for calibration in factory. The new structure will further reduce the resonator size and enhance miniaturization.

In order to detect a specific molecule sensitively, the corresponding sensor configuration (e.g., the microdisk size and the gap between the microdisk and waveguide) and the operating laser wavelength range, need to be designed, characterized, and optimized. Experimental methods for conducting these tasks are very time-consuming and costly. A flexible simulation model is highly desired.

The radiation transport in microcavity WGM resonators involves near field optics. Thus, Maxwell's electromagnetic (EM) theory has to be adopted. The Lorenz-Mie theory[12] and the first-order perturbation model[11] were previously used for analytical studies. The method of separation of variables[7] can also be utilized to solve the simplified version of Maxwell's equations - Helmholtz equation. The limitation of the theoretical models is that they can only be applied to reveal the individual intuitive resonance properties of the microcavity, but cannot expect to capture the coupling of the evanescent fields in the gap separating a microcavity and a light-delivery waveguide, and to investigate the interactions of resonator evanescent radiation field with surrounding media. As a matter of fact, signal strength in the microcavity is very sensitive against the gap through which photons tunnel between the waveguide and microcavity. A complete modeling of EM field in the whole structure of WGM resonators is needed.

The waveguide-microdisk coupling WGM resonator is of high quality factor and has high energy storage at the resonant frequency due to minimal reflection loss in small volume fabricated cavities. As the dimension of the microcavity decreases, however, thermal phenomena could be more inclined to result in side effects.[13] In general, the change in temperature influences the optical properties and dimension of the microcavity; and as a result, the resonant frequency may shift and thermal instability occurs. The thermal phenomena lead to the perturbation of the wavelength of the pumping light in microcavity laser and the change in the intensity of the resonance filed inside the microcavity. For example, thermal effects will influence the lasing stability of WGM-based microlasers and the sensitivity of WGM-based sensors. It is needed to investigate the thermal phenomena using multi-scale and multi-physical modeling.

In this first report, characterization of the WGM resonators is focused on the numerical studies of optical resonant phenomena under a broad range of WGM configuration parameters including microcavity size and gap. The resonators considered consist of a waveguide for light delivery and a microdisk as the cavity. They are manufacturable devices through optical lithography and conventional microelectronics techniques. The finite element method (FEM) is employed for the simulation. The operating resonant frequencies are chosen in the near infrared range, which is ideal for biomaterials and biomolecules. Research results regarding the size and gap effects and energy storage under resonances are presented.

THOERY AND SIMULATION

Electromagnetic model

WGM resonance inside the microdisk is typically an equatorial brilliant ring, and this ring is located on the same plane as the waveguide. So it is feasible to use a two-dimensional (2-D) theoretical model. The time-dependent Maxwell's equations are

$$\begin{cases} \nabla \cdot \bar{E} = \dfrac{\rho}{\varepsilon}; \quad \nabla \times \bar{E} = -\mu \dfrac{\partial \bar{H}}{\partial t} \\ \nabla \cdot \bar{H} = 0; \quad \nabla \times \bar{H} = \bar{J} + \varepsilon \dfrac{\partial \bar{E}}{\partial t} \end{cases} \tag{1}$$

where $\bar{E}$ and $\bar{H}$ are the electric and magnetic field vectors, respectively; ε and μ are the permittivity and permeability of the medium; ρ is the electric charge density; and $\bar{J}$ is the electric current density.

For the electric field, since $\rho = 0$ and $\bar{J} = \sigma \bar{E}$, we can derive the equation for $\bar{E}$ as follows:

$$\nabla^2 \bar{E} - \mu\sigma \frac{\partial \bar{E}}{\partial t} - \mu\varepsilon \frac{\partial^2 \bar{E}}{\partial t^2} = 0 \tag{2}$$

where σ is the electrical conductivity. We can transfer the above equation to the form of a time-harmonic wave by setting $\bar{E}(\bar{r}, t) = \bar{E}_0(\bar{r}) e^{i\omega t}$. The coupled set of Maxwell's equations is then reduced to a simple form:

$$\frac{1}{\mu}\nabla^2 \bar{E} + \omega^2 \varepsilon_c \bar{E} = 0; \quad \frac{1}{\mu}\nabla^2 \bar{H} + \omega^2 \varepsilon_c \bar{H} = 0 \tag{3}$$

where we have introduced the complex permittivity $\varepsilon_c = \varepsilon - i(\sigma/\omega) = \varepsilon_{cr}\varepsilon_0$ and $\omega = 2\pi c/\lambda$; ε_{cr} is the complex relative permittivity, ε_0 is the permittivity in vacuum, c is the speed of light in the medium, and λ is the light wavelength. ε_{cr} is calculated by $\varepsilon_{cr} = m^2 = n^2 - k^2 - i2nk$. Here, the complex index of refraction, $m = n - ik$, is conveniently introduced; n is the real part of the refractive index and represents a spatial phase change of the electromagnetic wave; k is the absorption index and stands for a spatial damping on the electromagnetic wave.

In the present study we consider the In-plane TE waves, where the electric field has only a z-component; and it propagates in the x-y plane. Thus, the fields can be written as:

$$\bar{E}(x,y,t) = E_z(x,y)\bar{e}_z e^{i\omega t}; \quad \bar{H}(x,y,t) = [H_x(x,y)\bar{e}_x + H_y(x,y)\bar{e}_y]e^{i\omega t} \tag{4}$$

At the interface and physical boundaries, the natural continuity condition is used for the tangential component of the magnetic field, i.e., $\bar{n}\times\bar{H}=0$. For the outside boundaries, the low-reflecting boundary condition is adopted. The low-reflecting means that only a small part of the wave is reflected, and that the wave propagates through the boundary almost as if it were not present. This condition can be formulized as $\bar{e}_z\cdot\bar{n}\times\sqrt{\mu}\bar{H}+\sqrt{\varepsilon}E_z=0$. The light source term E_{0z}, which propagates inwards through the entry of the waveguide, was treated as an electrically low-reflecting boundary expressed by

$$\bar{e}_z\cdot\bar{n}\times\sqrt{\mu}\bar{H}+\sqrt{\varepsilon}E_z = 2\sqrt{\varepsilon}E_{0z}. \tag{5}$$

The WGM resonances possess very high quality factors. The quality factor Q is defined as a ratio of 2π stored energy to energy lost per cycle. From the energy conservation and resonance properties, we can deduce a simple approximate expression:[14] $Q=\omega_0/\Delta\omega=2\pi\omega_0\tau$, where ω_0 is the resonant frequency, $\Delta\omega$ is the resonance linewidth, and τ is the photon lifetime.

Heat transfer model

Poynting's theory

From Maxwell's equations (1), we can derive the energy conservation equation to describe the resistive and radiative energy, or energy loss, through Poynting's theorem:[15]

$$\oint_S (\bar{E}\times\bar{H})\cdot\bar{n}dS = -\int_V\left(\bar{E}\cdot\frac{\partial\bar{D}}{\partial t}+\bar{H}\cdot\frac{\partial\bar{B}}{\partial t}\right)dV-\int_V\bar{J}\cdot\bar{E}dV \tag{6}$$

where V is the computation domain and S is the closed boundary of V. The term on the left had side of the above equation represents the radiative losses. The quantity $\bar{S}=\bar{E}\times\bar{H}$ is called as the Poynting vector. The first integral on the right hand side represents the rate of change in total energy. The second integral on the right hand side represents the resistive losses that result in heat dissipation in metallic materials.

For dielectric materials, however, $\bar{J}=0$. Under the assumption that the material is linear and isotropic we have constitutive relations as follows:

$$\bar{E}\cdot\frac{\partial\bar{D}}{\partial t}=\varepsilon\bar{E}\cdot\frac{\partial\bar{E}}{\partial t}=\frac{\partial}{\partial t}(\frac{1}{2}\varepsilon\bar{E}\cdot\bar{E}) \qquad \bar{H}\cdot\frac{\partial\bar{B}}{\partial t}=\frac{1}{\mu}\bar{B}\cdot\frac{\partial\bar{B}}{\partial t}=\frac{\partial}{\partial t}(\frac{1}{2\mu}\bar{B}\cdot\bar{B}) \tag{7}$$

So the formula of Poynting's theory is simplified to

$$\oint_S (\bar{E}\times\bar{H})\cdot\bar{n}dS = -\frac{\partial}{\partial t}\int\left(\frac{1}{2}\varepsilon\bar{E}\cdot\bar{E}+\frac{1}{2\mu}\bar{B}\cdot\bar{B}\right)dV \tag{8}$$

This formula shows us that the change in total energy of electromagnetic filed is totally converted to radiative energy. There is no heat dissipation in this condition. However, actual dielectric materials are dispersive (absorbing) media, and exhibit energy losses because the presence of dispersion in general signifies a dissipation of energy.

To discuss dispersion, let us consider an electromagnetic field of a single frequency. The differential form of equation (8) is expressed as $\nabla\cdot(\bar{E}\times\bar{H})=-(\bar{E}\cdot\frac{\partial\bar{D}}{\partial t}+\bar{H}\cdot\frac{\partial\bar{B}}{\partial t})$, in which the steady rate of change of the energy is the mean quantity Q of heat evolved per unit time and volume.[19]

Supposing $\bar{E}$ and $\bar{D}$ are complex numbers for a field of a single frequency, we substitute $(\bar{E}+\bar{E}^*)/2$ and $(-i\omega\varepsilon\bar{E}+i\omega\varepsilon^*\bar{E}^*)/2$ for $\bar{E}$ and $\partial\bar{D}/\partial t$ respectively [$\bar{D}^*=\varepsilon^*\bar{E}^*$ and $\bar{E}(\bar{r},t)=\bar{E}_0(\bar{r})e^{-i\omega t}$], and similarly for $\bar{H}$ and $\partial\bar{B}/\partial t$. After averaging with respect to time over the period $2\pi/\omega$, the products $\bar{E}\cdot\bar{E}$ and $\bar{E}^*\cdot\bar{E}^*$, which contain factors $e^{\mp 2i\omega t}$, give zero, leaving the rate of change in electromagnetic energy as

$$Q=(\bar{E}\cdot\frac{\partial\bar{D}}{\partial t}+\bar{H}\cdot\frac{\partial\bar{B}}{\partial t})=\frac{i\omega}{4}[(\varepsilon^*-\varepsilon)\bar{E}_0\cdot\bar{E}_0+(\mu^*-\mu)\bar{H}_0\cdot\bar{H}_0]$$
$$=\frac{\omega}{2}(\varepsilon''\bar{E}_0\cdot\bar{E}_0+\mu''\bar{H}_0\cdot\bar{H}_0) \tag{9}$$

where ε'' and μ'' are the imaginary parts of ε and μ. The energy loss Q should be positive $(Q>0)$ since the dissipation of energy is accompanied by the evolution of heat[16] (under the law of increase of entropy). It hints that the imaginary parts of ε and μ are always positive for all substance and at all frequencies.

Heat Conduction Model

For a homogeneous, isotropic solid with heat generation, the differential equation of conduction heat transfer can be written as[17]

$$\nabla\cdot[k\nabla T(\bar{r},t)]+g(\bar{r},t)=\rho C_p\frac{\partial T(\bar{r},t)}{\partial t} \tag{10}$$

Where $g(r,t)=Q$, that is predicted from equation (9); k is the thermal conductivity, ρ the density, and C_p the specific heat capacity. Convective heat transfer boundary condition can be applied around the cavity surface.

The heat conduction part has not yet been incorporated in the present calculations, but it will be considered in the future report.

Simulation method

Maxwell's equations can be solved by the finite-difference time-domain (FDTD) method.[18] The drawbacks of the FDTD method lie with the time consuming in obtaining stationary

solutions, the large memory requirement, and the staircase approximation in the treatment of irregular configurations. Thus, it is not very ideal for simulation-based optimal design purpose. More than 30 years ago, Silvester[19] developed high order Lagrange elements and first applied the finite element method (FEM) for solving EM field problems. The present authors[20] successfully applied the FEM to simulate the EM and radiation energy fields in the WGM resonators of microsphere and optical fiber coupling structure.

In the present EM simulation, the finite element method is employed and detailed description of the method is available in literature.[20,21] Thus, it is not repeated here. The commercial software FEMLAB was used for the finite element solution and for pre- and post-processing. A typical simulation model is similar to the left hand figure in Fig. 1. The simulation domain adopted is a 20μm × 25μm rectangular area with a centered microdisk as the resonant cavity. The length of the waveguide is extended to the edge of the simulation domain. A laser beam from a tunable continuous-wave (CW) laser is coupled into the left end of the waveguide to excite the resonance. The frequency of the incident laser varies between 365 THz (822nm) and 375 THz (800nm). When the frequency of the input light is the same as the natural resonant frequency of the system, WGM phenomenon occurs. At the resonant frequency, the scattering intensity from the microdisk will increase sharply and form a peak in the intensity-frequency spectrum.

In the simulation, the model geometry is generally meshed by 51,400 triangle elements. We also considered less triangle elements. The results for different meshes are consistent and the outputs from 51,400 triangle elements are satisfactory. The general computational resolution of wavelength is 0.5nm, but special attention is paid to the resonance frequency regions where 0.01nm resolution is adopted. To conduct parametric studies, the diameter of the microdisk varies between 10 and 15μm. The width of the waveguide changes between 2 and 3μm. The gap between the microdisk and the waveguide varies between 100 to 300nm.

RESULTS AND DISCUSSION

The present study is focused on the numerical characterization of microdisk-waveguide coupling microcavity WGM resonators for decision-making in the design of manufacturable WGM micro/nano-devices. The sketch of such a device is shown in Fig. 1. It is an integrated waveguide and microdisk photonic device to be fabricated on silicon wafers. Silicon Nitride (Si_3N_4) was selected as the material for the waveguide and microdisk because this substance has excellent physical and thermal stability, low cost,[22] and extremely low optical absorption around the operating wavelengths.[23] The thickness of the Si_3N_4 thin film is 1.3 μm. A 3μm-thick layer of SiO_2 is employed as the low cladding of the device. These thin films can be deposited on the surface of silicon wafer by using the low-pressure chemical vapor deposition (LPCVD) or the plasma-enhanced chemical vapor deposition (PECVD). The large refractive index of Si_3N_4 ensures high contrast of refractive indices between the WGM resonator and its surrounding medium (gas phase or aquous solutions) and may result in high-quality resonance modes. Figure 2 shows a SEM photo of a newly nanofabricated device using 248nm optical lithography and conventional silicon IC processing.

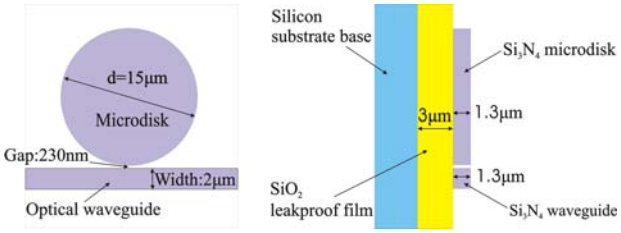

Figure 1. Sketch of a waveguide-microdisk coupling WGM resonator.

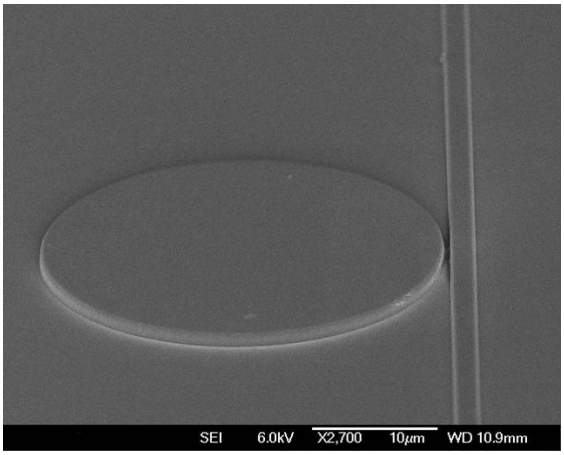

Figure 2. SEM photo of a fabricated WGM microcavity resonator (fabrication was conducted in collaboration with the NJ Nanotechnology Consortium at Bell Labs/Lucent Technologies).

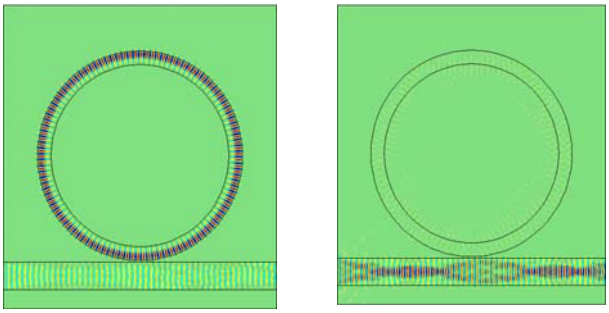

Figure 3. Electric field distributions under on-resonance (left hand side) and off-resonance (right hand side).

WGM resonances provide an excellent opportunity to observe micro/nanoscale radiation transport phenomena because of the enhancement of radiation field in small vicinity inward the cavity surface. First we try to demonstrate the great

difference of the EM field and radiation energy distributions between the on-resonance and off-resonance cases. Figures 3 and 4 illuminate the distributions of the electric field and the radiation energy density, respectively, for both off-resonance and first-order resonance for comparison purpose. The resonant frequency considered is at 373.78 THz (λ=802.61nm). The off-resonance frequency was selected at 372.67 THz (λ=805nm). The diameter of the microdisk is 15μm and the surrounding medium is air. The gap which is defined as the smallest distance between the waveguide and microdisk is 230nm and the width of the waveguide is 2μm. Both the microdisk and the waveguide are made from silicon nitride whose refractive index is assumed to be a constant of 2.01 against the operating wavelength.

In Fig. 3, it is clearly observed that the EM field exists in the microdisk no matter there is a WGM resonance or no resonance. Thus, photons tunnel from the waveguide to the microdisk because the gap distance is less than one wavelength. Under the first-order resonance, however, a brilliant ring in the EM field is formed inside the microdisk in the vicinity close to the peripheral surface. The strength in the ring is dozens of times stronger than that in the waveguide through where the excitation light is delivered. Under the off-resonance case, however, the strength of EM field in the waveguide is much stronger than that in the cavity.

From Fig. 4, it is seen that the microdisk and waveguide coupling resonator has an appealing energy storing property in the resonator when WGMs occur. The majority energy stores in the thin ring close to the peripheral surface of the microdisk under resonances. The ratio of the radiation energy storing in the microdisk to the radiation energy passing through the waveguide is found to be 10.5 for the first-order resonance shown in Fig. 4, whereas this ratio is only 0.008 for the case of off-resonance. The high energy storage in the small volume cavity leads to great enhancement of micro/nanoscale radiation field around the periphery of the resonator, where sensitivity to any external perturbation is maximal. As compared with the EM field and energy distribution results in our previous study[21] for WGM resonators with a microsphere and an eroded optical fiber coupling structure, we found that the new design of waveguide-microdisk coupling resonator has greatly improved the quality of WGM resonances. The ratio of the radiation intensity storing in the microsphere to the radiation intensity passing through the optical fiber was only 1.8 under the considered resonance in our previous study.

The gap effects on WGM resonators are shown in Figs. 5 - 7. Figure 5 shows the electric field for two similar WGM resonators with different gap distances, i.e. g = 200 and 400nm, respectively. They are working under the same mode (m = 118) of resonance. The comparison of the electric field was selected because it shows more obvious difference than the comparison of radiation energy distribution. It is observed that the EM field in the small gap resonator (g = 200) is stronger and more radiation energy is stored. However, it should not conclude that a small gap is better for WGM resonances because the resonance may be very weak in the case of zero gap distance. As a matter of fact, we found that, with the decrease of gap distance, the quality factor of the resonance decreases and the full width at half maximum (FWHM) of the resonant band increases, as shown in Fig. 6. The decrease of the gap results in a broadening in the FWHM of the resonant frequency band, and consequently reduces the quality factor and the finesse (defined by FSR/FWHM) of the resonant frequencies. However, the gap has only minor effect on the determination of resonant frequencies.

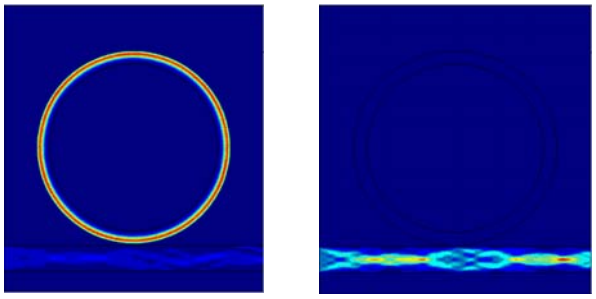

Figure 4. Energy distributions under on-resonance (left hand side) and off-resonance (right hand side).

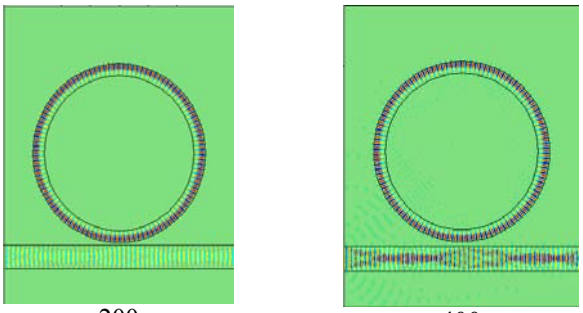

Figure 5. Comparison of electric field distribution with different gaps.

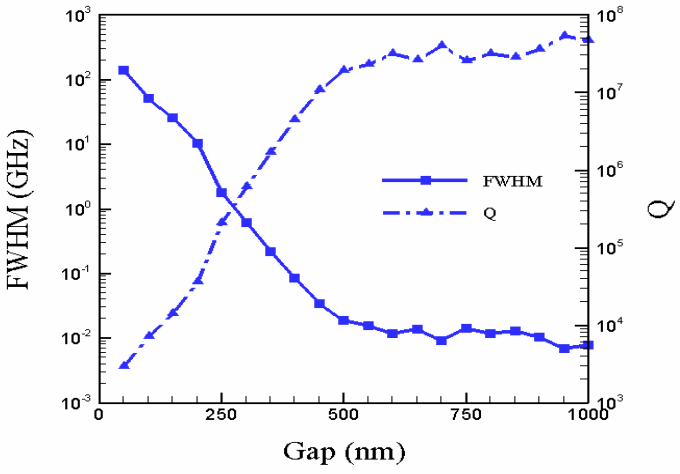

Figure 6. Gap effects on quality factor and FWHM.

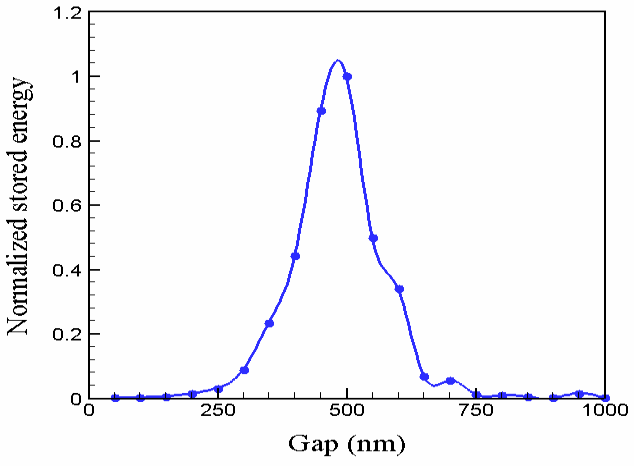

Figure 7. Stored energy (normalized) vs. gap distance.

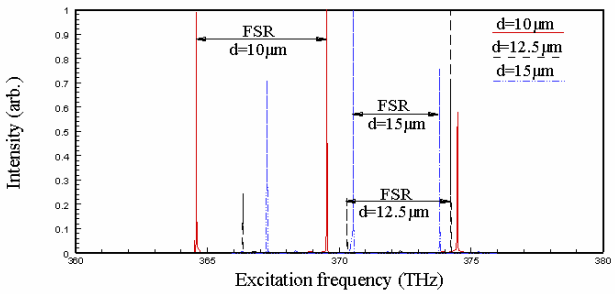

Figure 8. Scattering spectra for different microdisk sizes of d = 10μm, 12.5μm, and 15μm, respectively.

Comparison of the stored energy inside the microdisk under the same resonant mode for different gap distances (from 10nm to 500nm) is plotted in Fig. 7. The energy is normalized using the maximum stored energy found. The graph indicates that a gap in the range between 300 nm and 600nm has higher capacity of energy storage. The maximum capacity of energy storage is found at a gap distance around 480nm for the WGM resonator considered.

The size of microdisk certainly affects the resonance phenomena and signal intensity. Figure 8 shows the scattering spectra for three different microdisk diameters: 10μm, 12.5μm, and 15μm, respectively. The width of the waveguide and the gap between the waveguide and microdisk are fixed at 2μm and 230nm, respectively. Three first-order resonant frequencies (modes) were found for each of the microdisk sizes in the frequency range considered. It is seen that the microdisk size affects significantly the resonant frequencies and their intervals. The free spectral range (FSR, representing periodicity of resonance peaks) increases with the decrease of the diameter of the microdisk. The FSR of the resonant modes for the 15μm-diameter microdisk are slightly varying between 3.266 THz and 3.281 THz. Such a wide FSR make the WGM microcavity an excellent candidate for detection of trace gas using spectroscopy method. The WGM frequencies are dominantly determined by the microdisk diameter. However, it is found that the microdisk size does not appreciably influence the quality factor and the finesse of resonance.

CONCLUSIONS

The characteristics of waveguide-microdisk coupling WGM miniature resonators were investigated via simulation. The EM fields and radiation energy distributions in the resonators are obtained through solution of rigorous theory – Maxwell's equations. It is found that photon tunneling between the waveguide and microdisk exists. However, the tunneling is very weak under off-resonance conditions and the radiation energy is well confined inside the waveguide. When WGM resonance occurs, photon tunneling is greatly enhanced and significant radiation energy is stored in the microcavity. A very brilliant ring with strong EM field and high radiation intensity is found inward the peripheral surface of the microdisk under first-order resonance. The WGM resonant frequencies and their intervals are mainly determined by the microdisk diameter. The gap separating the waveguide and microdisk and the waveguide size have little effect on the resonant frequencies and their intervals. The FSR between two successive resonant modes can reach to several THz for the considered WGM microcavity resonators. The gap separating the microcavity and waveguide strongly influences the WGM resonance quality including the qualify factor, the FWHM, and the finesse of the resonant modes. The smaller is the gap, the stronger are the EM field and radiation energy storage in the resonating microcavity. With the reduction of gap distance, the quality factor decreases and the FWHM of the resonant band increases. The gap effect on energy storage is irregular. Generally, a gap in the range between 300nm and 600nm has higher capacity of energy storage. The maximum capacity of energy storage is found at a gap distance of 4800nm for the WGM resonator considered.

The theoretical base for analyzing thermal phenomena was presented. However, the studies on thermal effects have not been completed at this moment and they will be the focus of our next report in the near future.

ACKNOWLEDGMENTS

Z. Guo acknowledges the partial support of a 2003 - 2004 Academic Excellence Fund Award from Rutgers University and a NSF grant (CTS-0318001) to the project. Support of device fabrication from the New Jersey Nanotechnology Consortium (NJNC) is also appreciated.

REFERENCES

1. Arnold, S., 2001, "Microspheres, photonic atoms and the physics of nothing", *American Scientists*, **89**, 414-421.
2. Cai, M, Painter, Q., Vahala, K.J., and Sercel, P.C., 2000, "Fiber-couppled microsphere laser", *Opt. Lett.*, **25**, 1430-1432.
3. Little, B.E., Chu, S.T., Haus, H.A., Foresi, J., and Laine, J.P., 1997, "Microring resonator channel dropping filters", *J. Lightwave Tech.*, **15**, 998-1005.

4. Blom, F.C., van Dijk, D.R., Hoekstra, H.J., Driessen, A., and Popma, T.J.A., 1997, "Experimental study of integrated-optics micro-cavity resonators: toward an all-optical switching device," *Appl. Phys. Lett.*, **71**, 747-749.
5. Boyd, R.W., and Heebner, J.E., 2001, "Sensitive disk resonator photonic biosensor", *Appl. Opt.*, **40**, 5742-5747.
6. Schiller, S., and Byer, R.L., 1991, "High-resolution spectroscope of whispering gallery modes in large dielectric spheres," *Opt. Lett.*, **16**, 1138-1140.
7. Blair, S. and Chen, Y., 2001, "Resonant-enhanced evanescent-wave fluorescence biosensing with cylindrical optical cavities", *Appl. Opt.*, **40**, 570-582.
8. Vollmer, F., Braun, D., Libchaber, A., Khoshsima, M., Teraoka, I., and Arnold, S., 2002, "Protein detection by optical shift of a resonant microcavity", *Appl. Phys. Lett.*, Vol. 80, No. 21, pp. 4057-4059.
9. Boyd, R.W., and Heebner, J.E., 2001, "Sensitive disk resonator photonic biosensor", *Appl. Opt.*, **40**, 5742-5747.
10. Arnold, S., Khoshsima, M., Teraoka, I., and Vollmer, F., 2003, "Shift of whispering-gallery modes in microspheres by protein adsorption", *Opt. Lett.*, **28**, 272-274.
11. Teraoka, I., Arnold, S., and Vollmer, F., 2003, "Perturbation approach to resonance shifts of whispering-gallery modes in a dielectric microsphere as probe of a surrounding medium", *J. Opt. Soc. Am. B*, **20**, 1937-1946.
12. Barber, P.W. and Chang, P.K., 1988, "Optical effects associated with small particles", World Scientific, Singapore; New Jersey; Hong Kong.
13. Carmon, T., Yang, L., and Vahala, K.J., 2004, "Dynamical thermal behavior and thermal self-stability of microcavities", *Optics Express*, Vol. 12, No. 20, pp.4742-4750.
14. Yariv, A., 1997, *Optical electronics in modern communications*, 5th ed., Oxford U. Press, Oxford, UK.
15. Kovetz, A., 1990, "*The Principles of Electromagnetic Theory*, Cambridge University Press.
16. Laudau, L.D. and Lifshitz, E.M., 1960, *Electrodynamics of continuous media*, Pergamon Press Ltd., New York.
17. Özisik, M. N., 1993, *Heat conduction*, 2nd ed., John Wiley & Sons, Inc., New York.
18. Taflove, A. and Hagness, S.C., 2000, "Computational Electrodynamics: The Finite-Difference Time-Domain Method", 2nd ed., Artech House, Norwood, MA.
19. Silvester, P.P., 1969, "Finite element solution of homogeneous waveguide problems", *Alta Frequenza*, **38**, 313-317.
20. Quan, H. and Guo, Z., 2004, "Finite element analyses of near-field radiation and resonance frequency shift in WGM nanoscopic biosensors," *Heat Transfer Science and Technology* 2004 (Bu-Xuan Wang Ed.), pp. 101 – 108, Proc. of *the 6th International Symposium on Heat Transfer*, Beijing, China, June 15-19.
21. Quan, H. and Guo, Z., 2005, "Simulation of whispering-gallery-mode resonance shifts for optical miniature biosensors", *Journal of Quantitative Spectroscopy and Radiative Transfer*, Vol. 93, pp. 231-243.
22. Hsu, T.R, 2002, *MEMS & microsystems design and manufacture*, McGraw-Hill, New York.
23. Palik, E. D., 1985, *Handbook of optical constants of solids*, Academic Press, Orlando.